Theory of *s-d* Scattering in Dilute Magnetic Alloys. I. Perturbation Theory and the Derivation of the Low Equation

S. D. SILVERSTEIN AND C. B. DUKE
General Electric Research and Development Center, Schenectady, New York

(Received 23 February 1967)

Abrikosov's perturbation-theory treatment of the *s-d* problem is first reviewed and then generalized to derive an integral equation for the vertex part of the self-energy at nonzero temperature incorporating the effects of the non-spin-dependent impurity potential. The equation obtained is manifestly identical to Suhl's Low equation for the "energy-shell" scattering amplitude. Thus the analysis establishes the connection between the Green's-function diagrammatic techniques and the *S*-matrix dispersion theory used by Suhl. It is demonstrated explicitly that the Low equation reproduces the vertex function perturbation series at best to logarithmic accuracy in third and higher orders for a contact *s-d* interaction. Therefore, the Low equation itself may be derived from perturbation theory for $T \gtrsim T_K$, where T_K is the Kondo temperature.

I. INTRODUCTION

IN the early theoretical studies of metals doped with magnetic impurities, the simple model of a contact *s-d* exchange interaction[1–4] between the conduction electrons and the localized orbitals was sufficient to explain qualitatively many of the anomalous electronic properties of the magnetic alloy systems. These calculations were characteristically second-order perturbation theory with results independent of the sign of the exchange integral.

The next important theoretical steps in the understanding of the alloy systems were investigations into the criteria for the formation and stabilization of the localized moment itself.[5–8] With particular reference to the Anderson model[6] and its subsequent solution in the Hartree-Fock approximation, three important parameters determine the existence or nonexistence of localized moments for various impurity systems. These parameters are the density of states, the intra-atomic Coulomb repulsion between opposite spin electrons on the same localized orbital, and the mixing or hybridization interaction between the rigid conduction band wave functions and the localized orbitals. For certain ranges of these parameters, in particular for small hybridization, the Hartree-Fock ground state of the system exhibits a stable localized moment at zero temperature. Indeed, the model and its solution appeared quite convincing except for perhaps a few added restrictions imposed by going beyond the Hartree-Fock analysis.[9,10]

Kondo's[11] calculation of the anomalous resistivity greatly revived interest in the field. For the simple model of a contact interaction only, he found that in higher orders of perturbation theory for the scattering amplitude starting with the second Born approximation, there occurs a noncancellation of the Fermi factors which ultimately leads to a logarithmic divergence of the scattering amplitude at the Fermi surface and a $\ln T$ term in the resistivity. For an antiferromagnetic exchange interaction, the Zener-Ruderman-Kittel-Kasuya-Yosida (Z-R-K-K-Y) model extended to the next order in the perturbation-theory calculation of the resistivity gives results which reproduce qualitatively the anomalous resistance minimum observed experimentally.[12] The need for an antiferromagnetic exchange as opposed to the characteristically ferromagnetic atomic *s-d* exchange can be satisfied from the deformation of the wave functions due to the hybridization in the Anderson model.[13,14]

The necessity of extending Kondo's calculation beyond low-order perturbation theory was immediately recognized. Three different approaches have been followed by Abrikosov,[15] Suhl,[16] and Nagaoka.[17] Each of these calculations concluded that the divergence in the scattering amplitude disappears, but at the same time for an antiferromagnetic exchange at temperatures $T > T_K$, the original Kondo explanation of the resistance minimum is appropriate. The temperature $T_K \sim T_F \exp(-N/2J\rho(0))$ enters the theory in a natural way for a cutoff *s-d* model [i.e., approximate the nonlocal exchange integral $J(\mathbf{p}, \mathbf{p}') = J$ for $\xi_p, \xi_{p'} \in (-\epsilon_F, +\epsilon_F)$] $\rho(0)$ is the density of states at the Fermi surface, and T_F is the Fermi temperature.

[1] C. Zener, Phys. Rev. **81**, 440 (1951).
[2] M. A. Ruderman and C. Kittel, Phys. Rev. **96**, 99 (1954).
[3] T. Kasuya, Progr. Theoret. Phys. (Kyoto) **16**, 45 (1956).
[4] K. Yosida, Phys. Rev. **106**, 893 (1957); **107**, 396 (1957).
[5] P. de Faget de Cateljau and J. Friedel, J. Phys. Radium **17**, 27 (1956); J. Friedel, Can. J. Phys. **34**, 1190 (1956); J. Phys. Radium **19**, 573 (1958); Nuovo Cimento Suppl. **7**, 287 (1958); A. Blandin and J. Friedel, J. Phys. Radium **19**, 573 (1958).
[6] P. W. Anderson, Phys. Rev. **124**, 41 (1961).
[7] P. A. Wolff, Phys. Rev. **124**, 1030 (1961).
[8] A. M. Clogston, B. T. Matthias, M. Peter, J. J. Williams, E. Corenzwit, and R. C. Sherwood, Phys. Rev. **125**, 541 (1962).
[9] J. R. Schrieffer and D. C. Mattis, Phys. Rev. **140**, A1412 (1965).
[10] A. C. Hewson, Phys. Rev. **144**, 420 (1966).
[11] J. Kondo, Progr. Theoret. Phys. (Kyoto) **32**, 37 (1964).
[12] G. J. van den Berg, in *Proceedings of the IXth International Conference on Low-Temperature Physics* (Plenum Press, Inc., New York, 1965), p. 955.
[13] P. W. Anderson and A. M. Clogston, Bull. Am. Phys. Soc. **6**, 1241 (1961).
[14] J. R. Schrieffer and P. A. Wolff, Phys. Rev. **149**, 491 (1966).
[15] A. A. Abrikosov, Physics **2**, 5 (1965); **2**, 61 (1965).
[16] H. Suhl, Phys. Rev. **138**, A515 (1965); **141**, 483 (1966); Physics **2**, 39 (1965); Varenna Lectures 1966 (to be published).
[17] Y. Nagaoka, Phys. Rev. **138**, A112 (1965).

An important question to ask is whether T_K is in itself a meaning physical temperature or rather an artificial radius of convergence introduced by the nature of the approximations used in obtaining the solutions. Low-order perturbation calculations[18] of the susceptibility valid for $T>T_K$ indicate that the s-d exchange interaction acts to introduce a compensating electron polarization in the neighborhood of the impurity which serves to reduce the net moment. More detailed calculations[19] using approximate solutions to the self-consistent equations of motion, which perhaps are meaningful for $T<T_K$, imply that the susceptibility saturates in the low-temperature region. Extended conjectures based on these latter calculations suggest that some of the alloy systems which are traditionally treated as nonmagnetic in the sense of the Anderson-Hartree-Fock analysis can be interpreted alternatively in terms of a complete compensation of the impurity moment by the conduction electron polarization. It must be stressed, however, that these latter theoretical conjectures have no unequivocal experimental support, although the work of Geballe *et al.*[20] and Knapp[21] can be interpreted in light of the compensation effect.

The calculations "predicting" complete compensation of the impurity moment must at present be considered speculative because of the nonuniqueness of the truncation procedure in the equation of motion approach. To ensure a proper choice, the solutions must conform to some rigorous limiting value which is predetermined by the solution to a soluble model. The success of the Gorikov-Abrikosov[22] treatments of superconductivity are partially due to the fact that their particular truncations and solutions were designed to reduce to the original BCS result for the ground state. The solutions which they obtained below the superconducting transition temperature are not simply related by analytic continuation techniques to those characteristic of the normal state. In the s-d problem, the only thing we know with some reliability (beyond low-order perturbation theory) is Abrikosov's[15] high-temperature solution. Both Fisher[23] and Hamann[24] have shown that the corrected solutions to Nagaoka's[17] truncation procedure reduce to Abrikosov's high-temperature results for $T_F \gg T > T_K$. Here T_F is the Fermi temperature. For $T<T_K$ a different solution is obtained. The agreement with Abrikosov's high-temperature results are encouraging but the low-temperature solutions cannot be resolved unequivocally until they are either verified experimentally or theoretically determined by comparison with an exact solution of a soluble model for the ground state.

In an attempt to extend the original Kondo calculation to all orders in the logarithmic divergence, Abrikosov[15] made use of the finite temperature field-theoretic methods which have been proven successful in the studies of Fermi-liquid theory, electron-phonon interactions, etc. The virtue of this approach lies in its direct contact with perturbation theory so that the consequences of any approximations made can be immediately determined by comparison with the relevant low-order perturbation terms. Abrikosov, like Kondo, considered a contact interaction only in the dilute concentration limit. He found that he could sum the perturbation series if he restricted his solution *ab initio* to the domain of logarithmic accuracy. For the model chosen, the irreducible self-energy has an expansion of the form

$$\Sigma(\epsilon) = \sum_n \left(\frac{J}{\epsilon_F}\right)^n \left\{ c\left[a_{n2} \ln^{n-2} \frac{|\epsilon|}{\epsilon_F} + a_{n3} \ln^{n-3} \frac{|\epsilon|}{\epsilon_F} + \cdots a_{nn} \right] + c^2 \left[b_{n3} \ln^{n-3} \frac{|\epsilon|}{\epsilon_F} + \cdots b_{nn} \right] + \cdots \right\}. \quad (1.1)$$

The consideration of very dilute systems eliminates all the terms of order c^2 (concentration) and higher. Logarithmic accuracy, in addition, implies the correct evaluation of only the leading term in the logarithm for each order in perturbation theory. Therefore, for the nth order of perturbation theory we presumably can calculate the coefficients a_{n2}, but a_{n3} and all higher coefficients are undetermined. Abrikosov's expression for the self-energy is in the form $\sim J \ln^{-2} |\epsilon|/T_K$, while the corresponding transport coefficient go as $\ln^{-2} T/T_K$. Hence, the solutions appear to be singular at T_K. The reason for this is that we have discarded all terms of lower order in the logarithmic divergence by the original restriction to logarithmic accuracy. Given the freedom of logarithmic accuracy *ab initio*, the specific nature of the incorrectly determined terms can alter the analytic structure of the resulting solutions drastically. We therefore conclude that the constraint to logarithmic accuracy limits the applicability of the solutions to the high-temperature regime, $T>T_K$.

In this paper, we first review and generalize the Abrikosov perturbation-theoretic treatment of the s-d problem. We derive the integral equation for the vertex part of the self-energy at finite temperature incorporating the effects of the non-spin-dependent impurity potential. The results obtained are identical to Suhl's[16] Low equation for the "on-shell" scattering amplitude, thus establishing the connection between the Green's-function diagrammatic techniques and the S-matrix dispersion theory used by Suhl. We demonstrate

---

[18] K. Yosida and A. Okiji, Progr. Theoret. Phys. (Kyoto) **34**, 505 (1965).
[19] J. R. Schrieffer, J. Appl. Phys. **38**, 1143 (1967).
[20] T. H. Geballe, B. T. Matthias, A. M. Clogston, H. J. Williams, R. C. Sherwood, and J. P. Maita, J. Appl. Phys. **37**, 1181 (1966).
[21] G. S. Knapp, J. Appl. Phys. **38**, 1267 (1967).
[22] A. A. Abrikosov, L. P. Gorkov, and J. E. Dzyaloshinski, *Methods of Quantum Field Theory in Statistical Physics* (Prentice-Hall, Inc., Englewood Cliffs, New Jersey, 1963).
[23] K. Fisher, Phys. Rev. **158**, 613 (1967).
[24] D. R. Hamann, Phys. Rev. **158**, 570 (1967).

explicitly that the Low equation reproduces the vertex function perturbation series to logarithmic accuracy in third order, but at best gives the fourth and higher orders to logarithmic accuracy in the sense of Abrikosov's treatment. Therefore, from the point of view of perturbation theory, where the approximations are rather explicit in contrast with those made in the formal scattering treatment,[25] the Low equation itself may be derived in the region $T>T_K$. Hence, the analytic continuations[26,27] of the solutions to the Low equation to low temperatures, $T\lesssim T_K$, although well defined, are based on the use of the Low equation in a temperature region where it does not correctly represent the sum of the perturbation-theory diagrams. We furthermore show in a subsequent paper that a linear equation can be constructed which sums the relevant perturbation-theory diagrams to logarithmic accuracy and whose solutions exhibit a different analytic structure from those of the nonlinear equation. However, the vertex functions which satisfy either the linear or nonlinear integral equations are related to the self-energy only in the limit of logarithmic accuracy; whereas the above remarks indicate that the passage to this limit does nor suffice to uniquely define their analytic properties. These two facts suggest cause for a reappraisal of the applicability of the analytically-continued solutions of the Low equation to calculate either equilibrium or transport properties near or below T_K.

II. GREEN'S-FUNCTION PERTURBATION THEORY FOR DILUTE MAGNETIC IMPURITY SYSTEMS

The contents of this section will be devoted primarily to a review and minor extension of the Abrikosov[15] analysis of the *s-d* problem. Finite temperature techniques will be used throughout.

We consider the effect of a dilute, random distribution of magnetic impurities on the electronic properties of a metallic or semiconductor system, and assume that each of the impurities possesses a well-defined magnetic moment in the host matrix. The interaction of the impurities with the conduction electrons is characterized by an interaction Hamiltonian of the form

$$\mathcal{H}_{\rm int}=-N^{-1}\sum_{\mathbf{p},\mathbf{p}'}\{J_1(\mathbf{p}',\mathbf{p})\delta_{\alpha'\alpha}+J_2(\mathbf{p}',\mathbf{p})\,\boldsymbol{\sigma}_{\alpha'\alpha}\cdot\mathbf{S}_n\}\times C_{\mathbf{p}'\alpha'}{}^{\dagger}C_{\mathbf{p}\alpha}\exp[i(\mathbf{p}-\mathbf{p}')\cdot\mathbf{R}_n]. \quad (2.1)$$

Here $\boldsymbol{\sigma}_{\alpha'\alpha}$ are the matrix elements of the Pauli spin matrices; $\mathbf{R}_n$ is the nth impurity coordinate; $\mathbf{S}_n$ is the impurity spin operator; $J_1(\mathbf{p}',\mathbf{p})$ is the standard impurity potential which mixes the Bloch states due to the nonperiodicity of the lattice; and $J_2(\mathbf{p}',\mathbf{p})$ is the effective Coulomb exchange integral between the conduction and localized states incorporating hybridization effects.[13,14]

An important difference between the above interaction and the one, for example, between electrons and phonons is the appearance of the dynamical operator $\mathbf{S}_n$ which does not obey simple boson of fermion commutation relations. The coupling of the electrons to operator is the cause of the logarithmic divergences which appear in higher orders of perturbation theory. The angular momentum commutation relations,

$$[S_n{}^i,\,S_{n'}{}^j]=i\epsilon_{ijk}S_n{}^k\delta_{nn'}, \quad (2.2)$$

preclude the standard diagrammatic expansion in which the problem is divided into all possible two particle contractions via Wick's theorem. There have been a variety of "effective" Wick-type theorems developed to accommodate spin operators.[28] Abrikosov's "pseudofermion" representation is particularly convenient as it reduces the problem to one similar to the traditional diagrammatic calculations and, moreover, allows one to take into account the complications introduced by the cross terms in the simultaneous consideration of both exchange and nonspin-dependent potentials.

Abrikosov introduces the following representation for the impurity spin operators:

$$S_n{}^i=a_{n\beta'}{}^{\dagger}a_{n\beta}\langle\beta'\mid S^i\mid\beta\rangle. \quad (2.3)$$

Here $\langle\beta'\mid S^i\mid\beta\rangle$ are the matrix elements of the spin matrices:

$$\langle\beta'\mid S^z\mid\beta\rangle=\beta\delta_{\beta\beta'};\qquad \langle\beta'\mid S^{\pm}\mid\beta\rangle=\delta_{\beta',\beta\pm1}[(S\mp\beta)(S\pm\beta+1)]^{1/2}. \quad (2.4)$$

A summation convention will be used throughout for all repeated Cartesian and Zeeman indicies. The $a_{n\beta}{}^{\dagger}$ and $a_{n\beta}$ are the creation and annihilation operators for a pseudofermion field. They satisfy the equal-time anticommutation relations,

$$\{a_{n\beta},\,a_{n'\beta'}{}^{\dagger}\}=\delta_{nn'}\delta_{\beta\beta'};\qquad \{a_{n\beta},\,a_{n'\beta'}\}=0. \quad (2.5)$$

It is a simple matter to show that the angular momentum commutation relations Eq. (2.2) are satisfied by the pseudofermion representation.

We are interested primarily in the limit of dilute concentrations of magnetic impurities. The contributions to the self-energy from multiple scattering from a single impurity are linear in the concentration while the terms involving multiple scatterings from different impurities are proportional to higher powers of the concentration. It suffices, therefore, to consider the spin states associated with a single impurity. We characterize the spin state of the impurity by the occupation numbers of the pseudofermions. The general state in occupation number space is represented by

$$\mid n_{-S},\,n_{-S+1},\cdots,\,n_{S-1},\,n_S\rangle, \quad (2.6)$$

where each of the n's take on the values 0 or 1. Hence there are $2^{(2S+1)}$ orthogonal basis states associated with

[25] The three major approximations in the scattering theory are: single-channel unitarity, single-particle intermediate states, and the pole approximation to the left-hand cut in the Mandlestam representation.

[26] H. Suhl and D. Wong, Physics **3**, 17 (1967).

[27] H. Suhl, Phys. Rev. Letters **17**, 1140 (1966).

[28] See, for example, B. Giovannini, Sci. Papers Coll. Gen. Educ. Univ. Tokyo **15**, 49 (1965).

the occupation number space of a single spin in the pseudofermion representation. The manifold of occupation number space relevant to the computation of the spin averages are the $2S+1$ singly occupied states (the $2S+1$ permutations of $|1, 0, 0, \cdots, 0\rangle$). The spurious degrees of freedom are contributed by the vacuum state $|0, 0, \cdots, 0\rangle$, and the states of higher than single occupation, e.g., there are $(2S+1)!/[(2S-1)!2!]$ doubly occupied states (permutations of $|1, 1, 0, \cdots, 0\rangle$), and in general $(2S+1)!/((2S+1-m)!m!)$ states within the manifold corresponding to m occupied pseudofermions. Here, $0 \leq m \leq 2S+1$, where m is an integer. In the absence of a magnetic field the degree of degeneracy of each manifold is the binomial coefficient as illustrated. Abrikosov has devised a method of eliminating these spurious states. To do so, he assigns an arbitrary positive single-particle energy λ to the pseudofermions. The singly occupied states have an energy λ, the doubly occupied an energy 2λ, and the mth an energy $m\lambda$. The thermodynamic probability for occupation of the mth manifold is

$$\frac{(2S+1)!}{(2S+1-m)!m!}\frac{e^{-\lambda m/T}}{Z_s(T)}, \tag{2.7}$$

where the partition function $Z_s(T)$ is given by

$$Z_s(T) = \sum_{m=0}^{2S+1} \frac{(2S+1)!}{(2S+1-m)!m!} e^{-\lambda m/T} = [1+e^{-\lambda/T}]^{(2S+1)}. \tag{2.8}$$

In order to obtain the correct spin average, one includes an additional normalization factor $e^{\lambda/T}/(2S+1)$ and "freeze-out" the spurious states relative to the singly occupied states by always taking the limit $\lambda/T \to \infty$ when performing spin averages. After the limit is taken, the results are independent of the initial choice of λ. This procedure does not "freeze out" the physically relevant states relative to the vacuum as the operation of any product of spin operators on the vacuum state gives zero. The vacuum must, however, be included to preserve the cyclic invariance of the trace in performing the averages. The correct average of any function of single spin terms is therefore generated by

$$\langle f(\mathbf{S})\rangle = \lim_{\lambda/T\to\infty} \frac{e^{\lambda/T}}{2S+1} \times \mathrm{Tr}\Big[\exp\Big(-\sum_{-S}^{+S} \lambda \hat{n}_{\beta''}/T\Big) f(a_{\beta'}{}^{\dagger} a_{\beta} \langle \beta' | \mathbf{S} | \beta\rangle)\Big]. \tag{2.9}$$

The interaction Hamiltonian Eq. (2.1) can be expressed in terms of the pseudofermion representation as

$$\mathcal{H}_{\mathrm{int}} = -N^{-1} \sum_{\mathbf{p},\mathbf{p}'} \{J_1(\mathbf{p}', \mathbf{p})\delta_{\alpha'\alpha}\delta_{\beta'\beta} + J_2(\mathbf{p}', \mathbf{p})\sigma_{\alpha'\alpha}{}^{i} S_{\beta'\beta}{}^{i}\} \times a^{\dagger}_{n\beta'} a_{n\beta} C^{\dagger}_{\mathbf{p}'\alpha'} C_{\mathbf{p}\alpha} \exp[i(\mathbf{p}-\mathbf{p}')\cdot\mathbf{R}_n], \tag{2.10}$$

where the non-spin-dependent impurity potential is diagonal in the extended pseudofermion space.

In discussing the expansion of the self-energy, we restrict consideration to a subset of self-energy graphs.

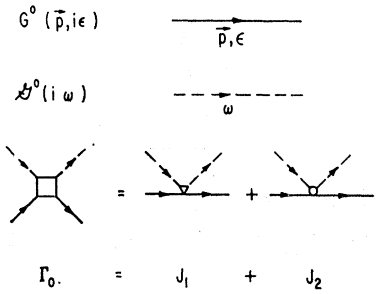

FIG. 1. Graphical representation of the free-electron propagator, free pseudofermion propagator, and the bare vertex function.

We do not consider the higher-order perturbation graphs incorporating renormalization of the pseudofermion propogator. In terms of a restricted s-d contact-interaction model, these graphs contribute terms of at least two orders lower in the logarithmic divergence for a given order of perturbation theory than the graphs considered. The self-energy graphs which are linear in the concentration are characterized by single closed pseudofermion loops, while multiple closed pseudofermion graphs exhibit powers in the impurity concentration equal to the number of closed loops. Hence, the multiple closed loop pseudofermion graphs will not be considered.

In the nth order of perturbation theory there will be various combinations of graphs corresponding to m J_1's and $(n-m)$ J_2's. In an nth order term in the expansion of the self-energy, the diagrams will be composed of $(n-1)$ free-electron propagators;

$$G_{\alpha\alpha'}{}^{0}(\mathbf{p}, i\epsilon) = \delta_{\alpha\alpha'}/i\epsilon - \xi_{\mathbf{p}'}, \qquad \epsilon = (2n+1)\pi T; \tag{2.11}$$

n pseudofermion propagators,

$$\mathcal{G}_{\beta\beta'}{}^{0}(i\omega) = \delta_{\beta\beta'}/i\omega - \lambda, \qquad \omega = (2l+1)\pi T; \tag{2.12}$$

all possible orderings of m J_1 electron-pseudofermion vertices, each represented by a triangle; and $(n-m)J_2$ vertices, each represented by a circle, as illustrated in Fig. 1. The λ in the denominator of the pseudofermion propagator corresponds to the arbitrary positive single particle pseudofermion energy used to eliminate the spurious states. As we recall, the elimination of the spurious states is always accomplished by taking the limit $\lambda/T \to \infty$ after all sums over Matsubara frequencies have been performed. The generation of the perturbation expansion with both J_1 and J_2 is rather cumbersome. It will suffice, for simplicity, to consider presently the perturbation expansion for $J_1 = 0$. The generalization to the full nonlocal Hamiltonian will be given later.

The lowest-order term in the expansion of the Green's function is represented by the diagram in Fig. 2. In the absence of a magnetic field, all diagrams exhibiting a pseudofermion loop of the form given in Fig. 2 will be zero as they arise from an equal time contraction of two pseudofermion operators and are always proportional

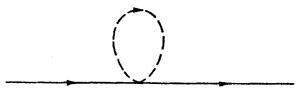

FIG. 2. Lowest-order term in the expansion of electron Green's function.

to terms of the form

$$\sum_{\beta} \langle \beta \mid S^i \mid \beta \rangle \mathcal{G}_{\beta\beta}(i\omega) = \mathcal{G}(i\omega)\ \mathrm{Tr}(S^i) = 0. \quad (2.13)$$

It is convenient to develop a simple nomenclature from which the subset of self-energy and vertex-function graphs considered can be specified. We specify the self-energy graphs by the symbol $\Sigma_{(1,2,3,\cdots n)}{}^{(i_1,i_2\cdots i_n)}$ where $(i_1, i_2, \cdots, i_n)$ is an arrangement of the integers $(1, 2, 3, \cdots n)$. In the self-energy graph, the electron propogates from $1\to 2\to 3\to\cdots n$, while the pseudofermion line propogates from $i_1\to i_2\to i_3\to\cdots i_n$. The $(n-1)!$ topologically distinct self-energy graphs for the nth order of perturbation theory are generated by the $(n-1)!$ noncyclic permutations of the pseudofermion indices. Each graph is invarient under a cyclic permutation. To illustrate this nomenclature, we consider the example of $\Sigma_{(123)}{}^{(132)}$ given in Fig. 3. Note, we always label the vertices with 1 starting at the left. The lower index denoting the electron propogation is suppressed with the convention that the electron always propogates from $1\to 2\to 3\cdots n$. We can illustrate the rules for computing the perturbation graphs by writing down the expression for this specific self-energy term:

$$\Sigma_{\alpha\alpha'}{}^{(132)}(\mathbf{p}, \mathbf{p}', i\epsilon) = \lim_{\lambda/T\to\infty} -\frac{e^{\lambda/T}}{2S+1} \langle \alpha \mid \sigma^i\sigma^j\sigma^k \mid \alpha' \rangle$$

$$\times \mathrm{Tr}(S^iS^kS^j) \frac{N_i}{N^3} \delta_{\mathbf{p},\mathbf{p}'}$$

$$\times \iint \frac{d^3p_1 d^3p_2}{(2\pi)^6} J_2(\mathbf{p}, \mathbf{p}_1) J_2(\mathbf{p}_1, \mathbf{p}_2) J_2(\mathbf{p}_2, \mathbf{p})\, T^2$$

$$\times \sum_{\omega_1\omega_2\omega_3} \mathcal{G}^0(i\omega_1)\mathcal{G}^0(i\omega_2)\mathcal{G}^0(i\omega_3)$$

$$\times G^0[\mathbf{p}_1, i(\epsilon+\omega_3-\omega_1)] G^0[\mathbf{p}_2, i(\epsilon+\omega_3-\omega_1)]. \quad (2.14)$$

We note that the order of the components of the S's relative to the σ's is specified by the labelling on the self-energy term. The i, j, k, indices refer to the Cartesian axis, where repeated indices are summed. In addition, there are (-1) factors for each closed fermion loop and each order of the interaction. The $\delta_{\mathbf{pp}'}$ comes from the average over the random positions of the impurities.

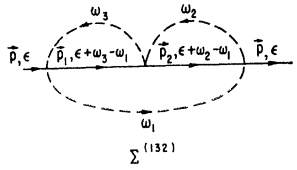

FIG. 3. The $\Sigma(\mathbf{p}, \epsilon)^{(123)}$ perturbation graph.

As an example of the method of calculation of the self-energy expressions at finite temperature, we review the second-order self-energy calculation. The only contributing second-order graph is shown in Fig. 4(a). The second-order self-energy contribution is

$$\Sigma_{\alpha\alpha'}{}^{(12)}(\mathbf{p}, i\epsilon) = \lim_{\lambda/T\to\infty} -\frac{e^{\lambda/T}}{2S+1} \langle \alpha \mid \sigma^i\sigma^j \mid \alpha' \rangle$$

$$\times \mathrm{Tr}(S^iS^j) \frac{N_i}{N^2} T^2 \sum_{\omega_1\omega_2} \times \int_{-\epsilon_F\le\xi_{\mathbf{p}'}} \frac{d^3p'}{(2\pi)^3} J_2(\mathbf{p}, \mathbf{p}') J_2(\mathbf{p}', \mathbf{p})$$

$$(i\omega_1-\lambda)^{-1}(i\omega_2-\lambda)^{-1}[i(\epsilon+\omega_2-\omega_1)-\xi_{\mathbf{p}'}]^{-1}. \quad (2.15)$$

The spin term is given by

$$\langle \alpha \mid \sigma^i\sigma^j \mid \alpha' \rangle\ \mathrm{tr}(S^iS^j) = \delta_{\alpha\alpha'} S(S+1)(2S+1). \quad (2.16)$$

The sums over the Matsubara frequencies ω_1, $\omega_2 = (2n+1)\pi T$ are now performed in the conventional manner.[15] For the ω_2 sum we have

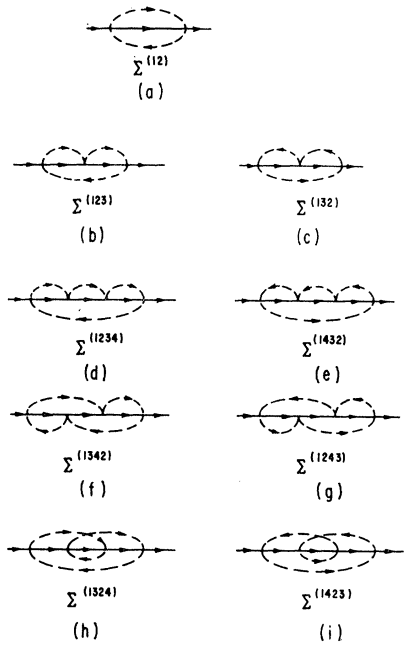

FIG. 4. The topologically distinct forms of the self-energy graphs considered through fourth order in the interaction.

$$T\sum_{\omega_2} [(i\omega_2-\lambda)(i(\epsilon+\omega_2-\omega_1)-\xi_{\mathbf{p}'})]^{-1}$$

$$= \frac{n(\lambda) - n(i(\epsilon-\omega_1)+\xi_{\mathbf{p}'})}{i(\epsilon-\omega_1)-\xi_{\mathbf{p}'}+\lambda}. \quad (2.17)$$

As $\epsilon-\omega_1 = 2l\pi T$, we obtain $n(i(\epsilon-\omega_2)+\xi_{\mathbf{p}'}) = n(\xi_{\mathbf{p}'})$. We note that the residue from the pole of the pseudofermion propagator is proportional to $n(\lambda)$ which goes as $e^{-\lambda/T}$ in the limit $\lambda/T\to\infty$. The contribution arises from the spurious pseudofermion states and will be "frozen out." We will retain the term here and discard it at the end of the calculation. More involved calculations are considerably simplified by only picking up the

pole contribution with the nonvanishing residues. The remaining sum in Eq. (2.15) can now be calculated:

$$[n(\lambda)-n(\xi_{p'})]T\sum_{\omega_1}[(i\omega_1-\lambda)(i(\epsilon-\omega_1)-\xi_{p'}+\lambda)]^{-1}$$

$$=\frac{[n(\lambda)-n(\xi_{p'})][n(\lambda)-n(i\epsilon-\xi_{p'}+\lambda)]}{i\epsilon-\xi_{p'}}. \quad (2.18)$$

Taking the limit $\lambda/T\to\infty$ using

$$\lim_{\lambda/T\to\infty} n(i\epsilon-\xi_{p'}+\lambda) = \lim_{\lambda/T\to\infty} n(i\pi T-\xi_{p'}+\lambda)$$

$$\to -e^{-\lambda/T}e^{\xi_{p'}/T}, \quad (2.19)$$

we obtain

$$\Sigma^{(12)}(\mathbf{p}, i\epsilon) = \lim_{\lambda/T\to\infty}\delta_{\alpha\alpha'}S(S+1)\frac{N_i}{N^2}$$

$$\times\int_{-\epsilon_F\le\xi_{p'}}\frac{d^3p'}{(2\pi)^3}J_2(\mathbf{p},\mathbf{p}')J_2(\mathbf{p}',\mathbf{p})(i\epsilon-\xi_{p'})^{-1}. \quad (2.20)$$

We finally analytically continue, $i\epsilon\to\epsilon+i\delta$ to obtain the *retarded* self-energy. For a contact interaction $J(\mathbf{p},\mathbf{p}')=$ J with cutoffs ξ_p, $\xi_{p'}\epsilon(-\epsilon_F, +\epsilon_F)$, the self-energy reduces to

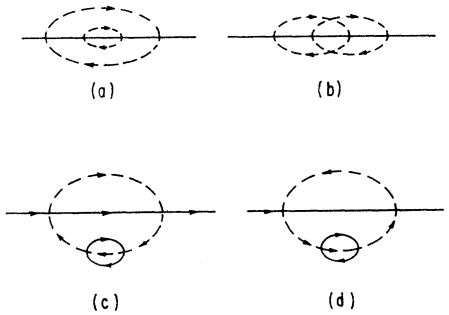

FIG. 5. Examples of fourth order self-energy graphs omitted. The forms: (a) and (b) are quadratic in the concentration; (c) and (d) are two orders lower in logarithmic divergence.

$$\Sigma^{(12)}(\mathbf{p},\epsilon)\cong -i\delta_{\alpha\alpha'}S(S+1)N_i(J/N)^2\rho(0)\pi;$$

$$\rho(0)=p_0m/2\pi^2. \quad (2.21)$$

The third-order self-energy is the lowest order in which the logarithmic divergence appears. It will suffice here to consider only the relevant diagrams for third and fourth order as shown in Figs. 4(b), 4(c), and 4(d)–(i), respectively, and illustrate the final result of the third-order self-energy calculations. The computations of higher-order vertex functions and self energies will be given in Appendix A. The third-order self-energy $\Sigma^{(132)}$, Eq. (2.16), is given for a contact interaction by

$$\Sigma_{\alpha\alpha'}{}^{(132)}(\mathbf{p},\epsilon) = -\delta_{\alpha\alpha'}\left(\frac{J}{N}\right)^3 N_i 2S(S+1)$$

$$\times\iint_{-\epsilon_F\le\xi_1,\xi_2\le\epsilon_F} d\xi_1 d\xi_2\frac{\rho(\xi_1)\rho(\xi_2)n(\xi_2)}{(\xi_1-\xi_2)(\epsilon-\xi_1+i\delta)}. \quad (2.22)$$

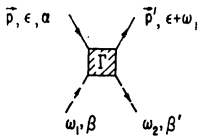

FIG. 6. The "four tailed" vertex function

$$\langle\alpha\beta\,|\,\Gamma[\mathbf{p}, i\epsilon; i\omega_1\,|\,\mathbf{p}', i(\epsilon+\omega_1-\omega_2), i\omega_2]\,|\,\alpha'\beta'\rangle.$$

Similarily, $\Sigma^{(123)}$ is given by

$$\Sigma_{\alpha\alpha'}{}^{(123)}(\mathbf{p},\epsilon)=\delta_{\alpha\alpha'}\left(\frac{J}{N}\right)^3 N_i 2S(S+1)$$

$$\times\iint_{-\epsilon_F\le\xi_1,\xi_2\le\epsilon_F} d\xi_1 d\xi_2\frac{\rho(\xi_1)\rho(\xi_2)n(-\xi_2)}{(\xi_1-\xi_2)(\epsilon-\xi_1+i\delta)}. \quad (2.23)$$

The total contribution in 3rd order is just the sum of these two expressions,

$$\Sigma_{3\alpha\alpha'}(\mathbf{p},\epsilon)=\delta_{\alpha\alpha'}\left(\frac{J}{N}\right)^3 N_i 2S(S+1)\iint_{-\epsilon_F\le\xi_1,\xi_2\le\epsilon_F} d\xi_1 d\xi_2$$

$$\times\frac{\rho(\xi_1)\rho(\xi_2)\tanh(\xi_2/2T)}{(\xi_1-\xi_2)(\epsilon-\xi_1+i\delta)}. \quad (2.24)$$

The term of leading order in the logarithmic divergence is attained by going to the zero temperature limit and projecting out the density of states terms at the Fermi surface,

$$\Sigma_{3\alpha\alpha'}(\mathbf{p},\epsilon)\cong -i\pi\delta_{\alpha\alpha'}(J/N)^3N_iS(S+1)\rho^2(0)$$

$$\times 4\ln(|\epsilon|/\epsilon_F).$$

In addition to the six fourth-order graphs generated by the 3! permutations of the pseudofermion indices, there are four graphs which are not included. These are illustrated in Fig. 5. The graphs in Figs. 5(a) and 5(b) are examples of those diagrams exhibiting multiple closed pseudofermion loops. These graphs are both quadratic in the impurity concentration, where each closed pseudofermion loop contributes a factor of the concentration. The graphs illustrated in Fig. 5(c) and 5(d) are the lowest-order contributions incorporating a renormalization of the pseudofermion propagator. These terms are at least two orders lower in the logarithmic divergence than the graphs which we have retained.

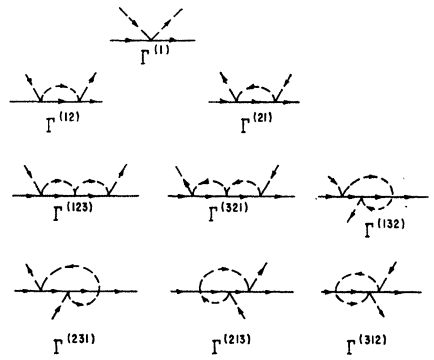

FIG. 7. The topologically distinct forms of the vertex function through third order in the interaction.

Vertex Part of the Self-Energy

In the calculation of the self-energy, we have generated the perturbation-expansion term by term but as yet have not developed a procedure to sum the graphs to infinite order. To facilitate this sum, we introduce the renormalized vertex which is represented by the graph in Fig. 6.

The renormalized "four-tailed" vertex function given in Fig. 6 corresponds to the sum of all possible graphs in which an electron line $\mathbf{p}$, ϵ, α enters and $\mathbf{p}'$, $\epsilon+\omega_1-\omega_2$, α' leaves; and a pseudofermion line ω_1, β enters and ω_2, β' leaves. We represent this vertex function by

$$\langle\alpha\beta \mid \Gamma(\mathbf{p}, i\epsilon; i\omega_1 \mid \mathbf{p}', i(\epsilon+\omega_1-\omega_2); i\omega_2) \mid \alpha'\beta'\rangle. \quad (2.25)$$

Our notation designates the entering and exiting lines by the left- and- right hand sides of the brackets, respectively. We now want to establish a nomenclature to specify the various topological forms of the vertex function which enter the perturbation expansion. We label the nth-order vertex function by the symbol

$$\langle\alpha\beta \mid \Gamma_{(1,2,3,\cdots n)}{}^{(i_1,i_2,\cdots i_n)} \times(\mathbf{p}, i\epsilon; i\omega_1 \mid \mathbf{p}', i(\epsilon+\omega_1-\omega_2); i\omega_2) \mid \alpha'\beta'\rangle. \quad (2.26)$$

Here the line ($\mathbf{p}$, ϵ, α) enters at 1, then propogates $1\rightarrow 2\rightarrow\cdots n$, where it exits as $\mathbf{p}'$, $\epsilon+\omega_1-\omega_2$, α'. The pseudofermion line enters at i_1, then propogates from $i_1\rightarrow i_2\rightarrow\cdots i_n$. In the nth order of perturbation theory there are $n!$ topologically distinct vertex-function graphs corresponding to the $n!$ arrangements of the pseudofermion indices relative to the fixed electron indices. We suppress the electron indices with the convention that the electron always follows the path $1\rightarrow 2\rightarrow 3\rightarrow\cdots n$. To illustrate this nomenclature, we consider examples through third order given in Fig. 7.

It can be shown that there is a one-to-one correspondence between each of the $n!$ vertex functions in the nth order, and each of the $n!$ topologically distinct self-energy graphs in the $(n+1)$th order,

$$\Sigma_{\alpha\alpha'}{}^{(1,i_2,i_3,\cdots i_{n+1})}(\mathbf{p}, i\epsilon) = \lim_{\lambda/T\rightarrow\infty} -\frac{e^{\lambda/T}}{2S+1} N_i T^2 \sum_{\omega_1\omega_2} \int_{-\epsilon_F\leq\xi_{p'}} \frac{d^3p'}{(2\pi)^3} \langle\alpha\beta \mid \Gamma_0(\mathbf{p}, \mathbf{p}') \mid \alpha'', \beta''\rangle \mathcal{G}^0(i\omega_1)\mathcal{G}^0(i\omega_2)$$
$$\times G^0[\mathbf{p}', i(\epsilon+\omega_2-\omega_1)]\langle\alpha''\beta'' \mid \Gamma^{(i_2,i_3,\cdots i_n)}[\mathbf{p}', i(\epsilon+\omega_2-\omega_1); i\omega_1 \mid \mathbf{p}, i\epsilon; i\omega_2]\mid \alpha'\beta\rangle. \quad (2.27)$$

This implies that the self-energy can be expressed in terms of the renormalized vertex by the graph illustrated in Fig. 8(a), where

$$\Gamma = \sum_{n=1}^{\infty} \sum_{\text{Perm}(i_1,i_2,\cdots i_n)} \Gamma^{(i_1,i_2,\cdots i_n)}; \quad (2.28a)$$

$$\sum(\mathbf{p}, i\epsilon) = \sum_{n=2}^{\infty} \sum_{\text{Perm}(i_2,i_3,\cdots i_n)} \Sigma^{(1,i_2,\cdots i_n)}(\mathbf{p}, i\epsilon). \quad (2.28b)$$

However, in order for Fig. 8(a) to be meaningful in summing all orders, we must obtain an integral equation for the full vertex function incorporating the variable dependence of all "four tails." No one has yet been successful in obtaining an integral equation for the full vertex function. Abrikosov circumvented this difficulty by considering the self-energy with both vertices "dressed" as illustrated in Fig. 8(b), but with a variable restriction on the functional dependence of the dressed vertices. He arrived at this result by adopting Eliashberg's[29] relations for $\text{Im}\Sigma^R(\mathbf{p}, \epsilon)$ used in the study of the damping of elementary excitations in a Fermi liquid. The expression for the imaginary part of the self-energy is equivalent to the optical theorem for the "on-shell" scattering amplitude. It is interesting to note that Eliashberg's derivation depends, in part, on the fact that $\text{Im}\Sigma^R(\mathbf{p}, \epsilon)\sim\epsilon^2$ for small ϵ. This behavior is exhibited by each term of the perturbation expansion in the interaction between the elementary excitations.[30] Such a behavior is not exhibited for impurity scattering in metals, and moreover, for s-d exchange scattering the individual terms in the perturbation expansion of $\text{Im}\Sigma^R(\mathbf{p}, \epsilon)$ diverge. Hence the applicability of the Fermi liquid relations to the s-d problem are not clear in a general sense. Abrikosov asserts that the double-dressed vertex graph correctly reproduces the self-energy to logarithmic accuracy. We have verified this assertion explicitly through fourth order in the contact s-d model.

If one were to accept the diagram in Fig. 8(b) literally without restricting the variable dependence of the vertices, it is a trivial matter to show from the previous discussion as illustrated by Eqs. (2.27), (2.28), that multiple counting of self-energy graphs occur, arising first in third order. These counting difficulties can be remedied to logarithmic accuracy by fixing the pseudofermion frequency variables appearing in the vertex function at the pole of the free pseudofermion propagator $i\omega_1$, $i\omega_2\rightarrow\lambda$. The expression for the

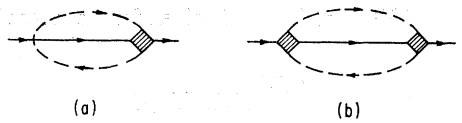

FIG. 8. (a) Proper self-energy represented by a single "dressed" vertex. (b) Self-energy represented by a double "dressed" vertex.

[29] G. M. Eliashberg, Zh. Eksperim. i Teor. Fiz. **42**, 1658 (1962) [English transl.: Soviet Phys.—JETP **15**, 1151 (1962)].

[30] J. M. Luttinger, Phys. Rev. **121**, 942 (1961).

self-energy is given by

$$\Sigma_{\alpha\alpha'}(\mathbf{p}, i\epsilon) \cong \lim_{\lambda/T\to\infty} -\frac{e^{\lambda/T}}{2S+1} N_i T^2 \sum_{\omega_1\omega_2} \int \frac{d^3q}{(2\pi)^3} \mathcal{G}^0(i\omega_1)\mathcal{G}^0(i\omega_2) G^0[\mathbf{q}, i(\epsilon+\omega_2-\omega_1)]$$
$$\times\langle\alpha\beta \mid \Gamma(\mathbf{p}, i\epsilon;\lambda \mid \mathbf{q}, i\epsilon;\lambda) \mid \alpha''\beta'\rangle\langle\alpha''\beta' \mid \Gamma(\mathbf{q}, i\epsilon;\lambda \mid \mathbf{p}, i\epsilon;\lambda) \mid \alpha'\beta\rangle. \quad (2.29)$$

The sums over the frequencies can now be performed in the standard manner and the results analytically continued to the region of real ϵ to obtain the retarded self-energy,

$$\mathrm{Im}\Sigma_{\alpha\alpha'}(\mathbf{p}, \epsilon) = -\frac{\pi N_i}{2S+1} \int \frac{d^3q}{(2\pi)^3} \delta(\epsilon-\xi_q) \langle\alpha\beta \mid \Gamma(\mathbf{p}, \epsilon+i\delta \mid \mathbf{q}, \epsilon+i\delta) \mid \alpha''\beta'\rangle\langle\alpha''\beta' \mid \Gamma(\mathbf{q}, \epsilon-i\delta \mid \mathbf{p}, \epsilon-i\delta) \mid \alpha'\beta\rangle. \quad (2.30)$$

The unitarity result $\mid \Gamma \mid^2$ is obtained by accounting for the overlapping cut structure in the external energy variable when performing the analytic continuations.[31,32] (See Appendix B.) The λ's in the vertex functions have been suppressed as the symmetric form $\Gamma(\mathbf{p}, \epsilon, \lambda \mid \mathbf{p}', \epsilon, \lambda)$ is independent of λ. From rotational symmetry we can write the general vertex in the form

$$\Gamma = \Gamma^{(S)} + (\boldsymbol{\sigma}\cdot\mathbf{S})\Gamma^{(V)}. \quad (2.31)$$

From this form we obtain

$$\langle\alpha\beta \mid \Gamma(\mathbf{p}, \epsilon+i\delta \mid \mathbf{q}, \epsilon+i\delta) \mid \alpha''\beta''\rangle\langle\alpha''\beta'' \mid \times\Gamma^*(\mathbf{p}, \epsilon+i\delta \mid \mathbf{q}, \epsilon+i\delta) \mid \alpha'\beta\rangle$$
$$= (2S+1)\delta_{\alpha\alpha'}[\mid \Gamma^{(S)}(\mathbf{p}, \epsilon \mid \mathbf{q}, \epsilon) \mid^2 + S(S+1) \mid \times\Gamma^{(V)}(\mathbf{p}, \epsilon, \mid \mathbf{q}, \epsilon) \mid^2]. \quad (2.32)$$

Inserting this into Eq. (2.30) we obtain the result

$$\mathrm{Im}\Sigma_{\alpha\alpha'}(\mathbf{p}, i\epsilon) = -\tfrac{1}{4}(N_i)\rho(\epsilon) \int d\xi_q d\Omega_{\mathbf{p}\cdot\mathbf{q}} \delta(\xi_q-\epsilon)$$
$$\times[\mid \Gamma^{(S)}(\mathbf{p}, \epsilon \mid \mathbf{q}, \epsilon) \mid^2 + S(S+1) \mid \Gamma^{(V)}(\mathbf{p}, \epsilon \mid \mathbf{q}, \epsilon) \mid^2]. \quad (2.33)$$

The problem to which we now address ourselves is the one of obtaining an integral equation for the vertex function which sums the perturbation series.

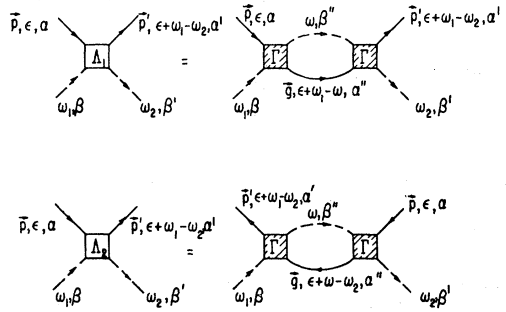

FIG. 9. Graphical equations for the electron vertex Λ_1, and the hole vertex Λ_2.

[31] L. D. Landau, Nucl. Phys. **13**, 181 (1959).
[32] J. S. Langer, Phys. Rev. **124**, 997 (1961).

III. GREEN'S-FUNCTION DERIVATION OF SUHL'S NONLINEAR LOW EQUATION FOR THE VERTEX FUNCTION

In this section we derive the nonlinear Low equation for the vertex function by Green's-function methods. The derivation is an extension of that of Abrikosov incorporating, in addition, the generalization to finite temperature and the use of the general nonlocal interaction described by Eq. (2.10). The resulting equation is identical to the nonlinear Low equation derived by Suhl using formal scattering theory. The primary advantage of a Green's-function derivation is that we establish direct contact with perturbation theory. Thus, the consequences of any approximations can be determined readily by direct comparison with the exact perturbation-theory results. We demonstrate that the Low equation reproduces perturbation theory to logarithmic accuracy in third order, but at best gives the fourth and higher orders to logarithmic accuracy when interpreted in terms of a contact-cutoff s-d model. The accuracy of the imaginary part of the self-energy in terms of the Green's-function expression Eq. (2.33), or alternatively in terms of the scattering amplitude in Suhl's treatment is similarly restricted.

In the nth order of perturbation theory for the s-d exchange term, there are $n!$ distinct topological forms for the vertex function, each being associated with the $n!$ distinct permutations of n spin operators. We seek an integral equation which will generate all of the distinct forms with each appropriately counted once. Let us first consider the integral equation given by Eq. (3.1) and by the diagrams in Fig. 9:

$$\Gamma = \Gamma_0 + \Lambda_1 + \Lambda_2, \quad (3.1)$$

Here Γ_0 is the bare vertex. The Λ_1 is called the electron vertex because the single-particle intermediate state lies above the Fermi energy. We can call Λ_2 the hole vertex because the intermediate energies lie below the Fermi energy. The integral equation, (3.1), is not correct for two reasons: First, the restriction to single particle-hole intermediate states precludes *ab initio*, the inclusion of any of the set of non "parquet" graphs, a simple example of which is given by the fourth-order graphs $\Gamma^{(2413)}$; $\Gamma^{(3142)}$, as illustrated in Fig. 10. For the

FIG. 10. Example of a fourth-order "nonparquet" graph.

cutoff *s-d* model, the nonparquet graphs within each order of perturbation theory are of a lower order in the logarithmic divergence. Hence, the use of single-particle intermediate states restricts the validity of the iterative results in fourth and higher orders to logarithmic accuracy. A second, more important aspect of the integral equation we have written is that the topological forms generated are multiply counted in higher-order iterations. This difficulty can also be remedied, but the restoration of proper counting, which brings us directly to the Low equation, further imposes the restriction to logarithmic accuracy in the iterative solution.

Let us first write out the expressions for Λ_1 and Λ_2 from the diagram in Fig. 9:

$$\langle\alpha\beta \mid \Lambda_1(\mathbf{p}, i\epsilon; i\omega_1 \mid \mathbf{p}', i(\epsilon+\omega_1-\omega_2); i\omega_2 \mid \alpha'\beta'\rangle = T\sum_{\omega}\int\frac{d^3q}{(2\pi)^3}$$
$$\times\mathcal{G}^0(i\omega)G^0[\mathbf{q}, i(\epsilon+\omega_1-\omega)]\langle\alpha\beta \mid \Gamma[\mathbf{p}, i\epsilon; i\omega_1 \mid \mathbf{q}, i(\epsilon+\omega_1-\omega]; i\omega] \mid \alpha''\beta''\rangle$$
$$\times\langle\alpha''\beta'' \mid \Gamma[\mathbf{q}, i(\epsilon+\omega_1-\omega); i\omega \mid \mathbf{p}', i(\epsilon+\omega_1-\omega_2); i\omega_2] \mid \alpha'\beta'\rangle; \quad (3.2a)$$

$$\langle\alpha\beta \mid \Lambda_2(\mathbf{p}, i\epsilon; i\omega_1 \mid \mathbf{p}', i(\epsilon+\omega_1-\omega_2); i\omega_2 \mid \alpha'\beta'\rangle = T\sum_{\omega}\int\frac{d^3q}{(2\pi)^3}$$
$$\times\mathcal{G}^0(i\omega)G^0[\mathbf{q}, i(\epsilon+\omega-\omega_2)]\langle\alpha\beta'' \mid \Gamma[\mathbf{p}, i\epsilon; i\omega \mid \mathbf{q}, i(\epsilon+\omega-\omega_2); i\omega_2]\alpha''\beta'\rangle$$
$$\times\langle\alpha''\beta \mid \Gamma[\mathbf{q}, i(\epsilon+\omega-\omega_2); i\omega_1 \mid \mathbf{p}', i(\epsilon+\omega_1-\omega_2); i\omega] \mid \alpha'\beta''\rangle. \quad (3.2b)$$

We now perform the sum over the Matsubara indices, $\omega=(2n+1)\pi T$. To do so, we must first analyze the analytic structure of the integrand as a function of the complex variable $z=i\omega$. In the complex z plane there is a simple pole at $z=\lambda$, and a line of singularities along $\mathrm{Im}[z-i(\epsilon+\omega_1)]=0$, which are contributed by the pseudofermion and electron Green's functions, respectively. In addition, there are series of multiple overlapping cuts along the lines $\mathrm{Im}z=0$; $\mathrm{Im}(z-i\epsilon)=0$, and $\mathrm{Im}(z-i(\omega_1-\omega_2))=0$, which are contributed by the vertex functions appearing in the integrand. This cut structure can be verified by an examination of the perturbation expansion of the vertex functions as illustrated in Appendix A. An important point to realize when performing the sum is that the contributions from the latter three cuts are all weighted by an additional $e^{-\lambda/T}$ factor relative to the contribution from the electron propogator. These contributions are reduced to zero when the spurious states are frozen out in the limit $\lambda/T\to\infty$. Hence, only the contributions from the electron propagator are of nonzero weight. The sum can now be simply performed. We obtain

$$\langle\alpha\beta \mid \Lambda_1[\mathbf{p}, i\epsilon; \omega_1 \mid \mathbf{p}', i(\epsilon+\omega_1-\omega_2); i\omega_2] \mid \alpha'\beta'\rangle = -\int\frac{d^3q}{(2\pi)^3}\frac{n(-\xi_q)}{i\epsilon-\xi_q-\lambda+iw_1}$$
$$\times\langle\alpha\beta \mid \Gamma[\mathbf{p}, i\epsilon; i\omega_1 \mid \mathbf{q}, \xi_q; i(\epsilon+\omega_1)-\xi_q] \mid \alpha''\beta''\rangle\langle\alpha''\beta'' \mid \Gamma[\mathbf{q}, \xi_q; i(\epsilon+\omega_1)-\xi_q \mid \mathbf{p}', i(\epsilon+\omega_1-\omega_2); i\omega_2] \mid \alpha''\beta'\rangle; \quad (3.3a)$$

$$\langle\alpha\beta \mid \Lambda_2[\mathbf{p}, i\epsilon; i\omega_1 \mid \mathbf{p}', i(\epsilon+\omega_1-\omega_2); i\omega_2] \mid \alpha'\beta'\rangle = -\int\frac{d^3q}{(2\pi)^3}\frac{n(\xi_q)}{i\epsilon-\xi_q+\lambda-iw_2}$$
$$\times\langle\alpha\beta'' \mid \Gamma[\mathbf{p}, i\epsilon; i(\epsilon+\omega_2-\xi_q) \mid \mathbf{q}, \xi_q; i\omega_2] \mid \alpha''\beta'\rangle\langle\alpha''\beta \mid \Gamma[\mathbf{q}, \xi_q; i\omega_1 \mid p', i(\epsilon+\omega_1-\omega_2); i(\epsilon+\omega_2)-\xi_q] \mid \alpha'\beta''\rangle. \quad (3.3b)$$

The $n(\xi_q)$'s in the above equations are Fermi factors, $(\exp(\xi_q/T)+1)^{-1}$.

As we recall from Sec. II, the vertex function relevant to the computation of one retarded self-energy was the analytically continued form

$$\Gamma(\mathbf{p}, \epsilon \mid \mathbf{p}', \epsilon) = \lim_{\substack{i\omega_1, i\omega_2\to\lambda\to 0\\ i\epsilon\to\epsilon}}\Gamma[\mathbf{p}, i\epsilon; i\omega_1 \mid \mathbf{p}', i(\epsilon+\omega_1-\omega_2); i\omega_2].$$

We note that we have set $\lambda=0$ only after all spurious pseudofermion states are "frozen out" of the problem. The results are, of course, completely independent of the initial choice of λ. Taking these limits, Eqs. (3.3) become

$$\langle\alpha\beta \mid \Lambda_1(\mathbf{p}, \epsilon \mid \mathbf{p}', \epsilon) \mid \alpha'\beta'\rangle = -\int\frac{d^3q}{(2\pi)^3}\frac{n(-\xi_q)}{\epsilon-\xi_q+i\delta}\langle\alpha\beta \mid \Gamma(\mathbf{p}, \epsilon+i\delta; 0 \mid \mathbf{q}, \xi_q; \epsilon-\xi_q) \mid \alpha''\beta''\rangle$$
$$\times\langle\alpha''\beta'' \mid \Gamma(\mathbf{q}, \xi_q; \epsilon-\xi_q \mid \mathbf{p}', \epsilon-i\delta; 0 \mid \alpha'\beta'\rangle; \quad (3.4a)$$

$$\langle\alpha\beta \mid \Lambda_2(\mathbf{p}, \epsilon \mid \mathbf{p}', \epsilon) \mid \alpha'\beta'\rangle = -\int\frac{d^3q}{(2\pi)^3}\frac{n(\xi_q)}{\epsilon-\xi_q+i\delta}\langle\alpha\beta'' \mid \Gamma(\mathbf{p}, \epsilon+i\delta; \epsilon-\xi_q \mid \mathbf{q}, \xi_q; 0) \mid \alpha''\beta'\rangle$$
$$\times\langle\alpha''\beta \mid \Gamma(\mathbf{q}, \xi_q; 0 \mid \mathbf{p}', \epsilon-i\delta; \epsilon-\xi_q) \mid \alpha'\beta''\rangle. \quad (3.4b)$$

The unitarity form, $\Gamma\Gamma^*$, exhibited in Eq. (3.4) arises from the consideration of the overlapping cut structure when performing the analytic continuations to obtain the retarded functions[32] (see Appendix B). The equation as it stands still suffers from multiple counting of the various topologically distinct vertex forms. As we will demonstrate explicitly from examples in third order, these counting inconsistencies can be remedied by placing the vertex functions appearing in the integrand of Eqs. (3.4) on the energy shell of the intermediate electron-hole propogator which reduces Eqs. (3.4) to the form

$$\alpha\langle\beta \mid \Lambda_1(\mathbf{p},\epsilon \mid \mathbf{p}',\epsilon) \mid \alpha'\beta'\rangle = -\int \frac{d^3q}{(2\pi)^3}\frac{n(-\xi_q)}{\epsilon-\xi_q+i\delta}\times\langle\alpha\beta \mid \Gamma(\mathbf{p},\xi_q \mid \mathbf{q},\xi_q) \mid \alpha''\beta''\rangle \times\langle\alpha''\beta'' \mid \Gamma^*(\mathbf{p}',\xi_q \mid \mathbf{q},\xi_q) \mid \alpha'\beta'\rangle; \quad (3.5a)$$

$$\langle\alpha\beta \mid \Lambda_2(\mathbf{p},\epsilon \mid \mathbf{p}',\epsilon) \mid \alpha'\beta'\rangle = -\int \frac{d^3q}{(2\pi)^3}\frac{n(\xi_q)}{\epsilon-\xi_q+i\delta}\times\langle\alpha\beta'' \mid \Gamma(\mathbf{p},\xi_q \mid \mathbf{q},\xi_q) \mid \alpha''\beta'\rangle \times\langle\alpha''\beta \mid \Gamma^*(\mathbf{p}',\xi_q \mid \mathbf{q},\xi_q) \mid \alpha'\beta''\rangle. \quad (3.5b)$$

From rotational symmetry, Γ can be divided into a scalar and a vector form

$$\Gamma=\Gamma^{(S)}+(\boldsymbol{\sigma}\cdot\mathbf{S})\Gamma^{(V)}. \quad (3.6)$$

Making use of Eqs. (3.1), (3.5), and (3.6) with the full nonlocal interaction (2.10), we obtain the coupled nonlinear integral equations for the scalar and vector vertex functions:

$$\Gamma^{(S)}(\mathbf{p},\epsilon \mid \mathbf{p}',\epsilon) = \frac{J_1(\mathbf{p},\mathbf{p}')}{N} - (4\pi N)^{-1}\int_{-\epsilon_F}^{\infty}\frac{\rho(\xi_q)d\Omega_{\mathrm{p}\cdot\mathrm{q}}d\xi_q}{\epsilon-\xi_q+i\delta} \times\{\Gamma^{(S)}(\mathbf{p},\xi_q \mid \mathbf{q},\xi_q)\Gamma^{(S)}(\mathbf{p}',\xi_q \mid \mathbf{q},\xi_q)^*+S(S+1)\Gamma^{(V)}(\mathbf{p},\xi_q \mid \mathbf{q},\xi_q)\Gamma^{(V)}(\mathbf{p}',\xi_q \mid \mathbf{q},\xi_q)^*\}; \quad (3.7a)$$

$$\Gamma^{(V)}(\mathbf{p},\epsilon \mid \mathbf{p}',\epsilon) = \frac{J_2(\mathbf{p},\mathbf{p}')}{N} - (4\pi N)^{-1}\int_{-\epsilon_F}^{\infty}\frac{\rho(\xi_q)d\Omega_{\mathrm{p}\cdot\mathrm{q}}d\xi_q}{\epsilon-\xi_q+i\delta} \times\{\Gamma^{(S)}(\mathbf{p},\xi_q \mid \mathbf{q},\xi_q)\Gamma^{(V)}(\mathbf{p}',\xi_q \mid \mathbf{q},\xi_q)^*+\Gamma^{(V)}(\mathbf{p},\xi_q \mid \mathbf{q},\xi_q)\Gamma^{(S)}(\mathbf{p}',\xi_q \mid \mathbf{q},\xi_q)^* -\tanh(\xi_q/2T)\Gamma^{(V)}(\mathbf{p},\xi_q \mid \mathbf{q},\xi_q)\Gamma^{(V)}(\mathbf{p}',\xi_q \mid \mathbf{q},\xi_q)^*\}. \quad (3.7b)$$

These coupled integral equations are manifestly identical to those derived by Suhl. It is important to note the consequence of the step in derivation which restored the proper counting, viz. putting the vertex functions in the integrand on the energy shell. This procedure has *forced* the vertex function to exhibit *no* singularities off of the real ϵ axis. From Eqs. (3.7) we see that the vertex function exhibits a line of singularities infinitesimally displaced below the real axis. We emphasize that this procedure generates the third-order graphs to logarithmic accuracy, but at best gives the fourth and higher orders to logarithmic accuracy[33] in terms of a restricted s-d cutoff model. Therefore, from the point of view of perturbation theory, the absence of singularities of $\Gamma(\mathbf{p},\epsilon \mid \mathbf{p}',\epsilon)$ in the upper half of the complex ϵ plane is a consequence of a variable substitution designed to compensate within logarithmic accuracy for the incorrect counting of certain diagrams.

In conclusion, we illustrate how the variable substitution $\epsilon\rightarrow\xi_q$ in the kernel of the integral equation restores the proper counting. For simplicity let us consider only a contact s-d interaction. We first discuss the topological forms generated by Eqs. (3.1) and (3.2). In second order we find

$$\Gamma_2=\Gamma^{(12)}+\Gamma^{(21)}. \quad (3.8)$$

In third order we find

$$\Gamma_3=2(\Gamma^{(123)}+\Gamma^{(321)})+\Gamma^{(132)}+\Gamma^{(231)}+\Gamma^{(213)}+\Gamma^{(312)}. \quad (3.9)$$

We now demonstrate how the variable substitution cancels the additional factor of two for the diagrams $\Gamma^{(123)}$ and $\Gamma^{(321)}$. The six topologically distinct third-order vertex functions can be written in the form

$$\Gamma^{(lmn)}(i\epsilon;i\omega_1 \mid i(\epsilon+\omega_1-\omega_2);i\omega_2) = c_{\mathrm{st}}{}^{(lmn)}(J/N)^3\iint_{-\epsilon_F}^{+\epsilon_F}d\xi_1 d\xi_2 I^{(lmn)}. \quad (3.10)$$

[33] Abrikosov has asserted that his calculation generates the leading order in the logarithmic divergence for all orders of perturbation theory. At present we have been unable to construct an *a priori* proof of his assertion for all orders. Our suspicions are further aroused by an apparent parodox presented by the linear theory derived in the succeeding paper. The linear integral equations for the vertex function omit a certain class of "parquet" diagrams, the lowest-order examples being $\Gamma^{(2143)}$ and $\Gamma^{(3412)}$ in fourth order. Nonetheless, the linear equation when solved for the contact s-d model gives the exact answer to logarithmic accuracy as that obtained by Abrikosov. We conclude that either Abrikosov's solution for the vertex function is not valid in fourth and higher orders, even to logarithmic accuracy, or alternatively the counting tricks used in the linear theory compensate for the omitted parquet diagrams. It appears that a partial resolution can be reached by an explicit calculation of the twenty-two parquet fourth-order vertex functions.

The factor $c_{\rm st}^{(lmn)}$ corresponds to the spin-term coefficient for the particular lmn form. For example,

$$c_{\rm st}^{(123)}=(\sigma^i\sigma^j\sigma^k)\,(S^iS^jS^k)$$
$$=\mathfrak{d}\cdot\mathbf{S}[S(S+1)+1]-S(S+1). \quad (3.11)$$

The expressions for all the vertex functions are given in Appendix A. To illustrate the counting, we consider the following examples of the integrals for $I^{(lmn)}$:

$$I^{(123)}=\frac{n(-\xi_1)n(-\xi_2)}{[i(\epsilon+\omega_1)-\xi_1-\lambda][i(\epsilon+\omega_1)-\xi_2-\lambda]}; \quad (3.12a)$$

$$I^{(132)}=\frac{n(-\xi_1)n(\xi_2)}{[i(\epsilon+\omega_1)-\xi_1-\lambda](-i\omega_2+\xi_1-\xi_2+\lambda)}; \quad (3.12b)$$

$$I^{(213)}=\frac{n(\xi_1)n(-\xi_2)}{[i(\epsilon+\omega_1)-\xi_2-\lambda](-i\omega_1+\xi_2-\xi_1+\lambda)}. \quad (3.12c)$$

We now analytically continue these forms, $i\epsilon\to\epsilon+i\delta$, $i\omega_1$, $i\omega_2\to\lambda+i\delta$ (see Appendices A and B) to obtain

$$I^{(123)}\to\frac{n(-\xi_1)n(-\xi_2)}{(\xi_1-\xi_2+i\delta)}[(\epsilon-\xi_1+i\delta)^{-1}-(\epsilon-\xi_2+i\delta)^{-1}]$$
$$=\frac{2n(-\xi_1)n(-\xi_2)}{(\epsilon-\xi_1+i\delta)\,(\xi_1-\xi_2)}; \quad (3.13a)$$

$$I^{(132)}\to\frac{n(-\xi_1)n(\xi_2)}{(\epsilon-\xi_1+i\delta)\,(\xi_1-\xi_2-i\delta)}; \quad (3.13b)$$

$$I^{(213)}\to\frac{n(\xi_1)n(-\xi_2)}{(\epsilon-\xi_2+i\delta)\,(\xi_2-\xi_1-i\delta)}. \quad (3.13c)$$

The integral equation previous to the variable substitution [e.g., Eq. (3.4)] generates two of the forms of $I^{(123)}$ as shown in Eq. (3.9). The act of substitution of ξ_q for ϵ in the vertex functions of the integrand of Eq. (3.4) to obtain correctly counted forms in Eq. (3.5) yields for the sum of the two contributions

$$\frac{2n(-\xi_1)n(-\xi_2)}{(\epsilon-\xi_1+i\delta)\,(\xi_1-\xi_2)}, \quad (3.14)$$

which is identical to the exact form (3.13a). Similarly, the Low equation generates the exact perturbation-theory term for $I^{(132)}$, but incorrect phases on the terms $I^{(231)}$ and $I^{(213)}$. The last forms generated by the Low equation are

$$I^{(231)}=\frac{n(\xi_1)n(-\xi_2)}{(\epsilon-\xi_1+i\delta)\,(\xi_1-\xi_2-i\delta)};$$

$$I^{(213)}=\frac{n(\xi_1)n(-\xi_2)}{(\epsilon-\xi_2+i\delta)\,(\xi_2-\xi_1+i\delta)}. \quad (3.15)$$

The discrepancy in the phase of $I^{(231)}$ and $I^{(213)}$ from the exact perturbation theory results does not alter the leading order term in the logarithmic divergence. The lower-order terms are, however, affected. In fourth order the situation is much more complicated. The results obtained for the fourth order vertex functions are *at best* accurate to logarithmic accuracy.[33]

We have shown that the iterative solutions to the nonlinear Low equation reproduces the exact perturbation theory for a contact *s-d* interaction at best only to leading order in the logarithmic divergence. The correction terms of lower order in the logarithmic divergence arise both from the omitted nonparquet graphs, and from the corrections to the energy-shell approximation procedure used to restore the proper counting of the most divergent terms alone.

APPENDIX A: PERTURBATION-THEORY CALCULATION OF VERTEX FUNCTIONS AND SELF-ENERGY

In this Appendix, we first compute the third-order vertex functions and then use these results together with Eq. (2.27) of the text to compute the fourth-order self-energy. We consider the simplest case of a contact *s–d* interaction:

$$J_1=0; \qquad J_2(\mathbf{p},\mathbf{p}')=J \qquad \text{for } \xi_{\rm p},\,\xi_{\rm p}'\in(-\epsilon_F,+\epsilon_F).$$

More elaborate integral equations for either the vertex function or the self-energy *must* reproduce both the real and imaginary parts of these results before it can be asserted that such equations possess an analytic structure compatible with that resulting from perturbation theory.

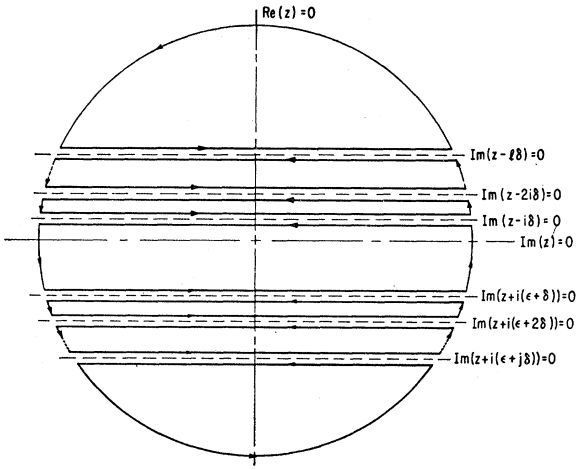

FIG. 11. The mapping of the integrand of Eq. (B2) into the complex z plane, and the closed contours C_μ taken to calculate the integral.

TABLE I. Tabulation of the third-order vertex functions.

(lmn)	c_{st}^{lmn}	$I^{lmn}[i\epsilon; i\omega_1 \mid i(\epsilon+\omega_1-\omega_2); i\omega_2]$	$I^{lmn}(\epsilon)$
(123)	$(\sigma^i\sigma^j\sigma^k)(S^iS^jS^k)=\mathfrak{d}\cdot\mathbf{S}[S(S+1)+1]-S(S+1)$	$\dfrac{n(-\xi_1)n(-\xi_2)}{[i(\epsilon+\omega_1)-\xi_1-\lambda][i(\epsilon+\omega_1)-\xi_2-\lambda]}$	$\dfrac{2n(-\xi_1)n(-\xi_2)}{(\epsilon-\xi_1+i\delta)(\xi_1-\xi_2)}$ [a]
(321)	$(\sigma^i\sigma^j\sigma^k)(S^kS^jS^i)=\mathfrak{d}\cdot\mathbf{S}[S(S+1)+1]+S(S+1)$	$\dfrac{n(\xi_1)n(\xi_2)}{[i(\epsilon-\omega_2)-\xi_1+\lambda][i(\epsilon-\omega_2)-\xi_2+\lambda]}$	$\dfrac{2n(\xi_1)n(\xi_2)}{(\epsilon-\xi_1+i\delta)(\xi_1-\xi_2)}$
(231)	$(\sigma^i\sigma^j\sigma^k)(S^iS^kS^j)=\mathfrak{d}\cdot\mathbf{S}[S(S+1)-1]-S(S+1)$	$\dfrac{n(\xi_1)n(-\xi_2)}{[i(\epsilon-\omega_2)-\xi_1-\lambda](i\omega_1+\xi_1-\xi_2-\lambda)}$	$\dfrac{n(\xi_1)n(-\xi_2)}{(\epsilon-\xi_1+i\delta)(\xi_1-\xi_2+i\delta)}$
(132)	$(\sigma^i\sigma^j\sigma^k)(S^iS^kS^j)=\mathfrak{d}\cdot\mathbf{S}[S(S+1)-1]+S(S+1)$	$\dfrac{n(-\xi_1)n(\xi_2)}{[i(\epsilon+\omega_1)-\xi_1-\lambda](-i\omega_2+\xi_1-\xi_2+\lambda)}$	$\dfrac{n(\xi_1)n(\xi_2)}{(\epsilon-\xi_1+i\delta)(\xi_1-\xi_2-i\delta)}$
(312)	$(\sigma^i\sigma^j\sigma^k)(S^kS^iS^j)=\mathfrak{d}\cdot\mathbf{S}[S(S+1)-1]-S(S+1)$	$\dfrac{n(-\xi_1)n(\xi_2)}{[i(\epsilon-\omega_2)-\xi_2+\lambda](i\omega_2+\xi_2-\xi_1-\lambda)}$	$\dfrac{n(-\xi_1)n(\xi_2)}{(\epsilon-\xi_2+i\delta)(\xi_2-\xi_1+i\delta)}$
(213)	$(\sigma^i\sigma^j\sigma^k)(S^jS^iS^k)=\mathfrak{d}\cdot\mathbf{S}[S(S+1)-1]+S(S+1)$	$\dfrac{n(\xi_1)n(-\xi_2)}{[i(\epsilon+\omega_1)-\xi_2-\lambda](-i\omega_1+\xi_2-\xi_1+\lambda)}$	$\dfrac{n(\xi_1)n(-\xi_2)}{(\epsilon-\xi_2+i\delta)(\xi_2-\xi_1-i\delta)}$

[a] Principle-value integrals are implied when phases are not specified.

We designate the third-order vertex function by

$$\Gamma^{(lmn)}[\mathbf{p}, i\epsilon; i\omega_1 \mid \mathbf{p}', i(\epsilon+\omega_1-\omega_2); i\omega_2] = c_{\rm st}{}^{(lmn)}\left(\frac{J}{N}\right)^3\int_{-\epsilon_F\le\xi_i\le\epsilon_F}\rho(\xi_1)d\xi_1\cdots\rho(\xi_3)d\xi_3 I^{(lmn)}[i\epsilon; i\omega_1 \mid i(\epsilon+\omega_1-\omega_2); i\omega_2]. \quad \text{(A1)}$$

The expressions for $c_{\rm st}{}^{(lmn)}$, $I^{(lmn)}[i\epsilon; i\omega_1 \mid i(\epsilon+\omega_1-\omega_2); i\omega_2]$ and its retarded form $I^{(lmn)}(\epsilon)$, $(i\omega_1, i\omega_2\to\lambda+i\delta)$ are given in Table I.

The fourth-order proper self-energy can now be obtained by using Eq. (2.27) of the text, i.e.,

$$\Sigma_{\alpha\alpha'}{}^{(1,l+1,m+1,n+1)}(\mathbf{p}, i\epsilon) = \lim_{\lambda/T\to\infty} -\frac{e^{\lambda/T}}{2S+1}\frac{N_i}{N}JT^2\sum_{\omega_1\omega_2}\int\frac{d^3q}{(2\pi)^3}\mathcal{G}^0(i\omega_1)\mathcal{G}^0(i\omega_2)G^0[\mathbf{q}, i(\epsilon+\omega_1-\omega_2)] \times\langle\alpha\beta \mid (\mathfrak{d}\cdot\mathbf{S})\Gamma^{(lmn)}[\mathbf{q}, i(\epsilon+\omega_1-\omega_2); i\omega_2 \mid \mathbf{p}, i\epsilon; i\omega_1] \mid \alpha'\beta\rangle. \quad \text{(A2)}$$

It suffices to illustrate one specific example and tabulate the results for the remaining contributions to the self-energy:

$$\Sigma_{\alpha\alpha'}{}^{(1234)}(\mathbf{p}, i\epsilon) = \lim_{\lambda/T\to\infty} -\frac{e^{\lambda/T}}{2S+1}\langle\alpha\beta \mid (\mathfrak{d}\cdot\mathbf{S})^4 \mid \alpha'\beta\rangle N_i\left(\frac{J}{N}\right)^4 T^2\sum_{\omega_1\omega_2}\int_{-\epsilon_F\le\xi_i\le\epsilon_F}\rho(\xi_1)d\xi_1\cdots\rho(\xi_3)d\xi_3 \times\{(i\omega_1-\lambda)(i\omega_2-\lambda)[i(\epsilon+\omega_1-\omega_2)-\xi_1]\}^{-1}\frac{n(-\xi_2)n(-\xi_3)}{[i(\epsilon+\omega_1)-\xi_2-\lambda][i(\epsilon+\omega_1)-\xi_3-\lambda]}. \quad \text{(A3)}$$

The ω_2 sum is readily performed leaving an ω_1 sum in the form

$$-T\sum_{\omega_1} 1/(i\omega_1-\lambda)\prod_{j=1}^{3}[i(\epsilon+\omega_1)-\xi_j-\lambda]^{-1}. \quad \text{(A4)}$$

In performing the ω_1 sum and subsequently analytically continuing to obtain the retarded function, we must account for the overlapping cut structure due to the ξ_i integrations. This sum is a specific example of the general result considered in Appendix B. We obtain

$$\Sigma_{\alpha\alpha'}{}^{(1234)}(\epsilon) = \delta_{\alpha\alpha'}S(S+1)[S(S+1)+1](J/N)^4N_i\int_{-\epsilon_F\le\xi_i\le\epsilon_F}\rho(\xi_1)d\xi_1\cdots\rho(\xi_3)d\xi_3 \times\sum_{l=1}^{3}(\epsilon-\xi_l+i\delta)^{-1}\prod_{j\neq l}^{3}\frac{n(-\xi_j)}{\xi_l-\xi_j+i\delta(j-l)}. \quad \text{(A5)}$$

The integrand of the above expression can be written in a more convenient form, after a suitable change of variables, as

$$\frac{\rho(\xi_1)\rho(\xi_2)\rho(\xi_3)n(-\xi_2)n(-\xi_3)}{\epsilon-\xi_1+i\delta}[3/(\xi_1-\xi_2)(\xi_1-\xi_3)-\pi^2\delta(\xi_1-\xi_2)\delta(\xi_1-\xi_3)]. \tag{A6}$$

A lack of specifications of phase, as illustrated by the first terms in the bracket of Eq. (A6), denotes a principal-value integral.

The contributions from the remaining fourth-order self-energies are evaluated in a similar manner. We obtain

$$\Sigma_{\alpha\alpha'}{}^{(l,m,n,o)}(\epsilon+i\delta)=-\Sigma_{\alpha\alpha'}{}^{(o,n,m,l)}(-\epsilon-i\delta), \tag{A7}$$

where

$$\Sigma_{\alpha\alpha'}{}^{(1243)}(\epsilon+i\delta)=\delta_{\alpha\alpha'}S(S+1)[S(S+1)-1]\left(\frac{J}{N}\right)^4 N_i\int_{-\epsilon_F\leq\xi i\leq\epsilon_F}\frac{\rho(\xi_1)d\xi_1\cdots\rho(\xi_3)d\xi_3}{(\xi_1-\xi_2)(\xi_1-\xi_3)}$$
$$\times\left\{\frac{2n(-\xi_2)n(\xi_3)}{\epsilon-\xi_1+i\delta}+\frac{n(-\xi_1)n(\xi_2)n(\xi_3)+n(\xi_1)n(-\xi_2)n(-\xi_3)}{\epsilon+\xi_1-\xi_2-\xi_3+i\delta}\right\}, \tag{A8}$$

and

$$\Sigma_{\alpha\alpha'}{}^{(1324)}(\epsilon+i\delta)=-\delta_{\alpha\alpha'}S(S+1)[S(S+1)-1](J/N)^4N_i\int_{-\epsilon_F\leq\xi i}\rho(\xi_1)d\xi_1\cdots\rho(\xi_3)d\xi_3$$
$$\times\left\{\frac{1}{(\xi_2-\xi_3)(\xi_1-\xi_3)}\left[\frac{2n(\xi_2)n(-\xi_3)}{\epsilon-\xi_1+i\delta}+\frac{n(-\xi_1)n(-\xi_2)n(\xi_3)+n(\xi_1)n(\xi_2)n(-\xi_3)}{\epsilon+\xi_3-\xi_2-\xi_1+i\delta}\right]\right.$$
$$\left.\frac{-\pi^2n(\xi_1)n(-\xi_1)\delta(\xi_1-\xi_3)\delta(\xi_2-\xi_3)}{\epsilon-\xi_1+i\delta}\right\}. \tag{A9}$$

Therefore, the total remaining part of the self-energy is given by

$$\Sigma_{\alpha\alpha'}{}^{(1243)}(\epsilon)+\Sigma_{\alpha\alpha'}{}^{(3421)}(\epsilon)+\Sigma_{\alpha\alpha'}{}^{(1324)}(\epsilon)+\Sigma_{\alpha\alpha'}{}^{(4231)}(\epsilon)$$
$$=2\delta_{\alpha\alpha'}S(S+1)[S(S+1)-1](J/N)^4N_i\int_{-\epsilon_F\leq\xi i\leq\epsilon_F}\frac{\rho(\xi_1)d\xi_1\cdots\rho(\xi_3)d\xi_3}{\epsilon-\xi_1+i\delta}$$
$$\times\left\{\frac{n(-\xi_2)n(\xi_3)+n(\xi_2)n(-\xi_3)}{(\xi_1-\xi_3)}[(\xi_1-\xi_2)^{-1}-(\xi_2-\xi_3)^{-1}]-\pi^2n(\xi_1)n(-\xi_1)\delta(\xi_1-\xi_2)\delta(\xi_1-\xi_3)\right\}. \tag{A10}$$

Finally, we compute the leading terms in the logarithmic divergence. The leading order in the logarithmic divergence is contributed by the imaginary parts of all terms considered. First, consider the contribution from $\Sigma^{(1234)}$ and $\Sigma^{(4321)}$. Taking the imaginary part, setting $T=0$, and projecting out the density of states at the Fermi surface, we obtain

$$\Sigma_{\alpha\alpha'}{}^{(1234)}(\epsilon)+\Sigma_{\alpha\alpha'}{}^{(4321)}(\epsilon)\cong-i\pi3S(S+1)[S(S+1)+1]\left(\frac{J}{N}\right)^4N_i\rho(\epsilon)\int_{-\epsilon_F}^{0}\rho(\xi_2)d\xi_2\int_{-\epsilon_F}^{0}\rho(\xi_3)d\xi_3$$
$$\times[1/(\xi_2-\epsilon)(\xi_3-\epsilon)+1/(\xi_2+\epsilon)(\xi_3+\epsilon)]\cong-i\pi6S(S+1)[S(S+1)+1](J/N)^4N_i\rho(0)^3\ln^2(|\epsilon|/\epsilon_F). \tag{A11}$$

In the evaluation of the remaining contributions, (A10), the relevant integrals are of the form

$$\int_0^{\epsilon_F}\rho(\xi_2)d\xi_2\int_{-\epsilon_F}^{0}\rho(\xi_3)d\xi_3[(\xi_2-\epsilon)(\xi_3-\epsilon)]^{-1}\cong-\rho(0)^2\ln^2\frac{|\epsilon|}{\epsilon_F} \tag{A12}$$

and

$$\int_{-\epsilon_F}^{0}\rho(\xi_2)d\xi_2\int_0^{\epsilon_F}\rho(\xi_3)d\xi_3[(\xi_2-\xi_3)(\epsilon-\xi_3)]^{-1}\cong\frac{\rho(0)^2}{2}\ln^2\frac{|\epsilon|}{\epsilon_F}. \tag{A13}$$

Hence,

$$\Sigma_{\alpha\alpha'}{}^{(1243)}(\epsilon)+\Sigma_{\alpha\alpha'}{}^{(3421)}(\epsilon)+\Sigma_{\alpha\alpha'}{}^{(1324)}(\epsilon)+\Sigma_{\alpha\alpha'}{}^{(4231)}(\epsilon)\cong i\pi\delta_{\alpha\alpha'}6S(S+1)[S(S+1)-1](J/N)^4N_i\rho(0)^3\ln^2\frac{|\epsilon|}{\epsilon_F}. \tag{A14}$$

The complete fourth-order result to logarithmic accuracy is the sum of (A11) and (A14),

$$\Sigma_{4\alpha\alpha'}(\epsilon)\cong-i\pi\delta_{\alpha\alpha'}12S(S+1)(J/N)^4N_i\rho(0)^3\ln^2(|\epsilon|/\epsilon_F). \tag{A15}$$

APPENDIX B: MATSUBARA SUMS AND ANALYTIC CONTINUATIONS OF INTEGRALS CONTAINING OVERLAPPING CUTS

In this Appendix, we illustrate the analytic continuation methods used to account for the overlapping cut structure which is often encountered in the Matsubara sums. As a general example, we consider an integral of the form

$$I(i\epsilon)=T\sum_{\omega=(2n+1)\pi T}\int d\xi_1\cdots d\xi_n h(\xi_1,\cdots\xi_n)\prod_{j=1}^{N_1}\frac{1}{i\omega-f_j}\prod_{l=1}^{N_2}(i\omega+i\epsilon-g_l)^{-1}. \tag{B1}$$

Here $f_j=f_j(\xi_1, \xi_2\cdots\xi_2)$ and $g_l=g_l(\xi_1, \xi_2\cdots\xi_n)$ are real linear combinations of the various ξ_i. We convert this sum to a contour integral in the complex $z=i\omega$ plane. The integrand in (B1), viewed as a function of the complex variable $z=i\omega$ possesses N_1, overlapping cuts along the line $\mathrm{Im}z=0$; and N_2 overlapping cuts along $\mathrm{Im}(z+i\epsilon)=0$. In performing the ω sum, we must separate the overlapping cuts. $I(i\epsilon)$ can be written as a contour integral

$$-\sum_{\mu}(2\pi i)^{-1}\oint_{C_\mu}dz n(z)\int d\xi_1\cdots d\xi_n h(\xi_1,\cdots\xi_n)\prod_{j=1}^{N_1}(z-f_j-ij\delta)^{-1}\prod_{j=1}^{N_2}(z+i\epsilon-g_l+il\delta)^{-1}. \tag{B2}$$

In Eq. (B2), $n(z)$ is the fermi function and the closed contours C_μ are indicated schematically in Fig. 11. The overlapping cuts have been displaced from each other by integral multiples of $i\delta$. The contour integral reduces to the sum of the line integrals along the cuts, for which we obtain the contributions

$$\int_{-\infty}^{+\infty}dz\Bigg\{\sum_{m=1}^{N_1}n(z)\prod_{l=1}^{N_2}(z+i\epsilon-g_l)^{-1}\prod_{j<m}(z-f_j+i\delta)^{-1}\prod_{j>m}(z-f_j-i\delta)^{-1}\delta(z-f_m)$$
$$+\sum_{k=1}^{N_2}n(z-i\epsilon)\prod_{j=1}^{N_1}(z-i\epsilon-f_j)^{-1}\prod_{l<k}(z-g_l-i\delta)^{-1}\prod_{l>k}(z-g_l+i\delta)^{-1}\delta(z-g_k)\Bigg\}, \tag{B3}$$

which is equal to

$$\sum_{m=1}^{N_1}n(f_m)\prod_{l=1}^{N_2}(f_m-g_l+i\epsilon)^{-1}\prod_{j\neq m}^{N_1}[f_m-f_j+i\delta(m-j)]^{-1}+\sum_{k=1}^{N_2}n(g_k-i\pi T)\prod_{j=1}^{N_1}(g_k-f_j-i\epsilon)^{-1}\prod_{l\neq k}^{N_2}[g_k-g_l-i\delta(k-l)]^{-1}. \tag{B4}$$

We next perform the analytic continuation to obtain the retarded function $I^R(\epsilon)$ accounting for the overlapping cuts due to the ξ_i integrations in (B2). Consider a general function of the form

$$F(z)=\int d\xi_1\cdots d\xi_n h(\xi_1,\cdots\xi_n)\prod_{j=1}^{N}(z-f_j)^{-1}, \tag{B5}$$

which exhibits N overlapping cuts at $\mathrm{Im}z=0$. $F(z)$ can be expressed in terms of the Cauchy integral

$$F(z)=\sum_{\nu}\oint_{C_\nu}\frac{dz}{2\pi i}\frac{F(z')}{z'-z}, \tag{B6}$$

where the contours C_ν are taken around the displaced cuts in a fashion analogous to that indicated in Fig. 11. The contributions from the line integrals are given by

$$F(z)=\int d\xi_1\cdots d\xi_n h(\xi_1,\cdots\xi_n)\sum_{m=1}^{N}(z-f_m)^{-1}\prod_{j\neq m}[f_m-f_j+i(m-j)\delta]^{-1}. \tag{B7}$$

The above result is independent of the sign of δ, because the overlapping cuts can be displaced in any order relative to each other. We analytically continue to obtain the retarded function

$$F^R(\epsilon)=\int d\xi_1\cdots d\xi_n h(\xi_1,\cdots\xi_n)\sum_{m=1}^{N}(\epsilon-f_m+i\delta)^{-1}\prod_{j\neq m}^{N}[f_m-f_j+i(m-j)\delta]^{-1}. \tag{B8}$$

The technique illustrated above is applied to (B4) to obtain, after some algebra, the result

$$I^R(\epsilon)=\int d\xi_1\cdots d\xi_n h(\xi_1,\cdots\xi_n)\times\sum_{k=1}^{N_2}\sum_{m=1}^{N_1}\frac{n(f_m)-n(g_k-i\pi T)}{\epsilon+f_m-g_k+i\delta}\prod_{j\neq m}^{N_1}[f_m-f_j+i(m-j)\delta]^{-1}\prod_{l\neq k}^{N_2}[g_k-g_l-i(k-l)\delta]^{-1}. \tag{B9}$$